J Mater Sci (2016) 51:4379–4389
DOI 10.1007/s10853-016-9750-9

# Preparation, characterization, and thermo-mechanical properties of poly (ε-caprolactone)-piperazine-based polyurethane-urea shape memory polymers

**Alireza Eyvazzadeh Kalajahi[1] · Mostafa Rezaei[1] · Farhang Abbasi[1]**

Received: 8 December 2015 / Accepted: 13 January 2016 / Published online: 21 January 2016


**Abstract** A series of segmented polyurethane-urea (PUU) shape memory polymers were synthesized from poly ε-caprolactone (PCL)-diol, hexamethylene diisocyanate, and piperazine (PP) with different hard to soft segment ratios. Chemical structure of PUUs was characterized using hydrogen nuclear magnetic resonance and attenuated total reflective-Fourier transform infrared spectroscopy methods. The results confirmed the formation of urethane and urea groups as well as incorporation of PP ring into polymer chain. Differential scanning calorimetry and wide angle X-ray scattering analyses were conducted to study the thermal properties and crystalline morphology of PUUs. It was found that crystallization of PUUs originated from PCL crystals. The reduction in degree of crystallinity was also observed with increasing of hard segment content (HSC). Mechanical properties were examined by tensile test at two different temperatures; above and below the PCL melting temperature. It was revealed that the chemical composition and temperature greatly affect the mechanical behavior of PUUs. A correlation between mechanical properties and physical structure of PUUs was established. Shape memory properties of PUUs were studied at two different programming processes. All of the samples show shape recovery over 94 % with a broad recovery temperature ranging from 40 to 65 °C. However, the shape fixity showed a great dependence on both HSC and programming process. The reasons of this dependency were discussed.

✉ Mostafa Rezaei
rezaei@sut.ac.ir

[1] Institute of Polymeric Materials, Polymer Engineering Department, Sahand University of Technology, Tabriz, P.O.Box 51335-1996, Iran

## Introduction

Shape memory polymers (SMPs) have attracted a great deal of interest in the last two decades due to their outstanding properties such as low density, good processability, high recoverable strain, ease in tailoring of thermo-mechanical properties, excellent chemical stability, biocompatibility, and even biodegradability [1–3]. SMPs are capable to store a temporary shape and return to their original shape in a predefined way by application of a proper stimulus such as temperature, water, light, and electrical or magnetic fields [4–7]. This unique property provides a good opportunity for the use of SMPs in biomedicine especially minimally invasive surgery. In such applications, SMP is fixed in a small temporary shape and after implantation in a suitable place in the body, returns to its applicable shape under a proper stimulus. However, for biomedical applications, the SMPs must have some important characteristics such as biocompatibility, biodegradability, high shape recoverability, and a recovery temperature near the human body temperature [8–12].

Biodegradable segmented polyurethane (PU) and polyurethane-urea (PUU) SMPs are a group of the advanced smart biomaterials which can have tunable mechanical and shape memory properties, depending on initial ingredients used for their synthesis. Segmented PUs and PUUs are composed of alternating soft and hard segments and show phase separated structure due to the thermodynamic incompatibility of the two segments [13, 14]. In biodegradable PUs and PUUs, the soft segment is generally based on poly (ε-caprolactone) (PCL), lactides, glycolide, and their copolymers. This soft segment serves as thermal switches for fixing the temporary shape; as well as hard segments which are formed by reaction of the isocyanate and the chain

extender (diols in PUs and diamines at PUUs), act as physical cross-links to retain initial shape [15–19].

Phase morphology, mechanical, and shape memory properties of PUs and PUUs greatly depend on the type and amount of polyols in soft segments as well as type of isocyanate and chain extender in hard segments [20–27]. Aromatic diisocyanates such as methylene diphenyl diisocyanate (MDI) and toluene diisocyanate (TDI) can lead to high shape memory and mechanical properties but unfortunately on degradation, they release carcinogenic and mutagenic materials which limit their use in biomedical applications [28, 29]. Using of aliphatic diisocyanates such as hexamethylene diisocyanate (HDI) can resolve this problem but in this case the mechanical properties decline substantially [30, 31]. Using diamines as chain extender is an alternative method for improvement of mechanical properties. Diamines introduce urea groups in hard segment phase which provide high number of hydrogen bonds and higher hydrogen bond energies in polymer chains. As well as urea groups lead to lower products acidity on degradation due to their basic nature and regulate the degradation rate [32–34]. However primary diamines are highly reactive due to their four reactive hydrogens per molecule and consequently may introduce crosslinking reactions during polymerization which reduce mechanical and shape memory properties. Use of secondary diamines with two reactive hydrogens per molecule may have advantage in best controlling of PUUs synthesis process. Piperazine (PP) can be a good choice for this purpose because it has a ring structure and its incorporation in polymer chain can enhance mechanical and shape memory properties of polymer. Furthermore PP as a standard drug intermediate has a good biocompatibility and does not affect polymer biocompatibility [35–37].

Based on our knowledge no appreciable study has been done on shape memory and mechanical properties of PUUs synthesized with PCL soft segment and PP/HDI hard segment. Thus the main goal of this study is the preparation of PUUs with PP as a chain extender with different hard segment contents (HSC). The HSC was controlled by PCL molecular weight and the molar ratio of hard to soft segments. We also characterized the chemical structure, thermal characteristics, mechanical properties, and shape memory behavior of PUUs using hydrogen nuclear magnetic resonance ($^1$H NMR) and attenuated total reflective-Fourier transform infrared (ATR-FTIR) spectroscopy methods, differential scanning calorimetry (DSC) and wide angle X-ray scattering (WAXS), tensile test, and two different shape memory programming processes. Furthermore, the effect of deformation temperature on shape memory and initial recovery temperature was studied. A good correlation between structure and mechanical and shape memory properties was established.

## Experimental

### Materials

ε-caprolactone (for synthesis, purity >98 %, Merck, Germany), stannous octoate (purity ≥96 %, Alfa Aesar, USA), PP (for synthesis, purity ≥99 %, Merck, Germany), and HDI (for synthesis, purity ≥99 %, Merck, Germany) were used as received. 1,4-butandiol (for synthesis, purity ≥98 %, Merck, Germany) was dried over 4 Å molecular sieves. Toluene (purity ≥99 %, Merck, Germany) was distilled over sodium under reduced pressure and stored over 3 Å molecular sieves before use. Isopropanol (purity ≥99 %, Merck, Germany) and *n*-hexane (purity ≥95 %, Merck, Germany) were used without further treatment.

### Polymer synthesis methods

#### *PCL-diol synthesis*

PCL-diol (Scheme 1a) was synthesized according to the procedure described elsewhere [38]. As representative for synthesize of PCL-diol with molecular weight of 2000 g/mol, stannous octoate (0.0248 g, $6.14 \times 10^{-5}$ mol) as catalyst and 1,4-butandiol (1.127 g, 0.0125 mol) as co-catalyst were initially added to a 250-ml four-necked glass flax equipped with thermocouple, condenser, and a magnetic stirrer, under nitrogen purge. Reaction vessel was placed in an oil bath at 90 °C for 30 min and then ε-caprolactone (50 g, 0.438 mol) was added to reaction mixture. Temperature of oil bath was raised to 120 °C and polymerization reaction was continued for extra 16 h. Finally synthesized PCL polymer was precipitated in *n*-hexane and dried under vacuum at 50 °C for 24 h.

#### *Polyurethane-urea synthesis*

A two-step polymerization method was employed for synthesis of PUUs. A predetermined amount of dried PCL-diol was initially dissolved in anhydrous toluene (10 % W/V) under nitrogen purge in a 250-ml three-necked round-bottomed flask equipped with thermocouple, condenser, and a magnetic stirrer. The reaction mixture was heated up to 80 °C for 20 min. A given amount of HDI and one drop of stannous octoate were added to solution and the reaction was continued for 3 h for prepolymer formation (Scheme 1b). In the second step, the reaction system was placed in an ice bath and then the dissolved PP in isopropanol mixture, was slowly added to the reaction system for chain extension reaction (Scheme 1c). Finally, the synthesized polymer was precipitated in *n*-hexane and post-cured at 100 °C for 24 h. The samples were nominated as PUU-M-RRR where M and R-R-R were used for PCL-diol molecular weight and isocyanate-chain extender-PCL molar ratios, respectively.

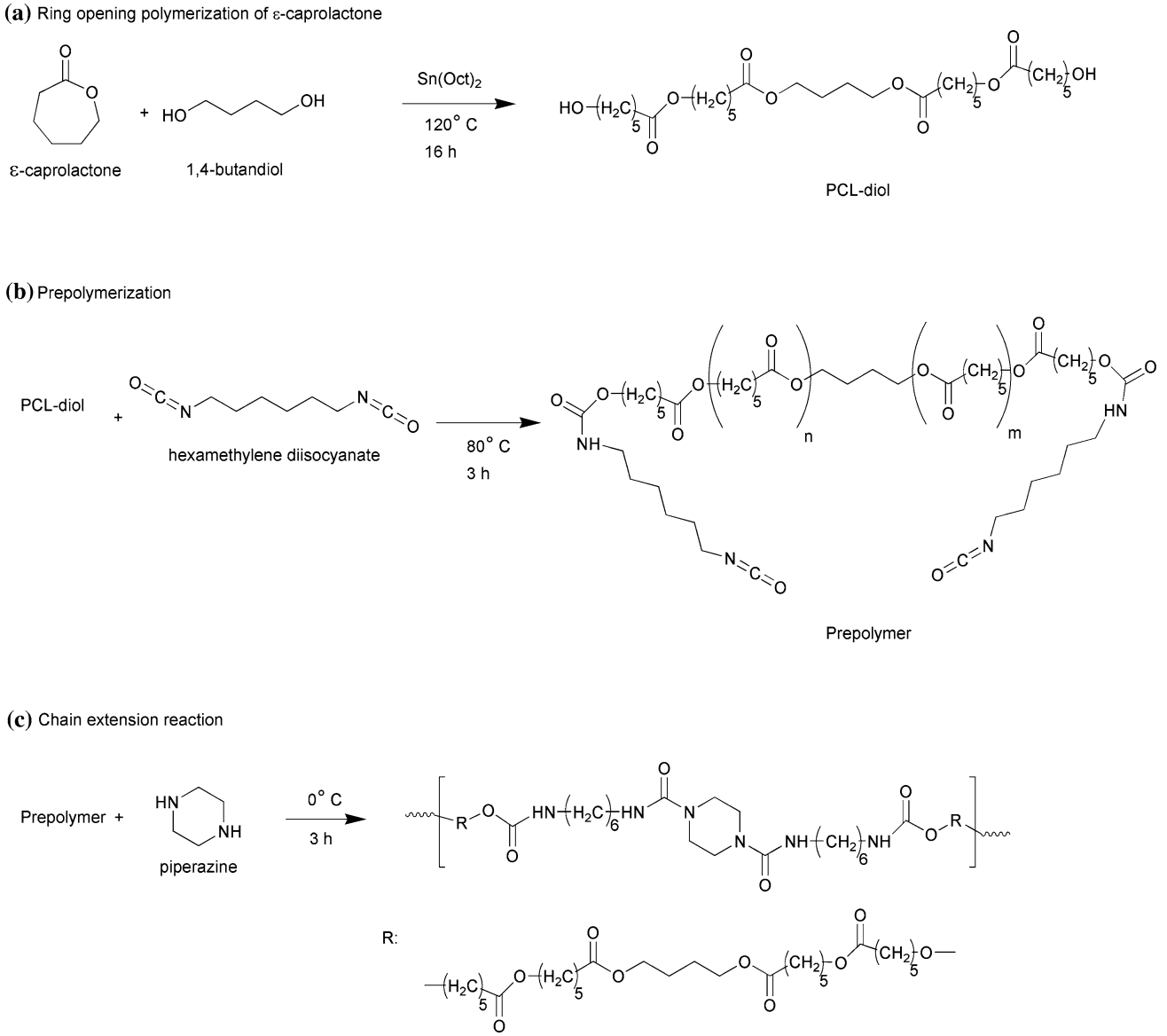


**Scheme 1** Synthesis of PCL-diol, prepolymer, and polyurethane-urea polymer (see text for details)

## Characterization

$^1$H NMR spectra of the PCL-diols and PUUs were recorded using a $^1$H NMR spectrometer (type Ultrashield 400 from Bruker, Germany). The samples were dissolved to 10 wt% in deuterated chloroform (CDCl3) and $^1$H NMR chemical shifts were measured with respect to tetramethylsilane (TMS) as internal standard.

Fourier transform infrared (FTIR) spectra were recorded on a FTIR spectrophotometer (type Tensor 27 from Bruker, Germany) in the range from 400 to 4000 cm$^{-1}$. Measurements were carried out on thin compression-molded films, using the attenuated total reflectance (ATR) technique. Each sample was scanned 24 times with a resolution of 4 cm$^{-1}$.

DSC was performed on a DSC apparatus (type DSC822 from Mettler-Toledo, Switzerland), over the temperature range of −20 to 100 °C under nitrogen atmosphere. A procedure with three runs of first heating, cooling, and second heating was applied to determine the melting and crystallization temperature of PCL soft segment in PUUs at a heating and cooling rate of 10 °C/min. Crystallinity percentage of soft PCL segment in PUUs was measured from the heat of fusion at first heating run ($\Delta H_{ml}$) and using a heat of fusion of 136 J/g for 100 % crystalline PCL [39].

Wide-angle X-ray diffraction (WAXS) patterns of PUUs were recorded by a X-ray diffractometer (type D5000 from Siemens, Germany) equipped with a scintillation counter and Cu Kα radiation ($\lambda = 0.1540$ nm) at an accelerating

voltage of 35 kV and a current of 20 mA. The measurements were performed in the range of $2\theta$ from 10° to 35° at a rate of 0.03 s/step. Degree of crystallinity of PUUs were obtained from graphical integration on the diffracted intensity data in the $2\theta$ range from 10° to 40° and subtracted from the amorphous scattering band intensity.

Tensile properties were measured according to ISO 527-2 using dumbbell shape specimen (type 5B), prepared by compression molding. Testing was conducted in tensile test machine (type Z010 from Zwick/Roell, Germany) equipped with 10 KN load cell. Specimens were kept at room condition (25 °C and 65 % relative humidity) for 2 weeks before test. Tensile properties were the average of at least three specimens. The strain of the samples was measured using the crosshead strain gauge of the tensile machine.

Shape memory properties of the samples were examined by means of tensile testing machine (type Z010 from Zwick/Roell, Germany). Two shape memory programming methods with different initial deformation temperatures (Room temperature and 60 °C) were conducted. For this purpose, the samples were initially stretched to 100 % strain, $\varepsilon_m$, at a rate of 20 mm/min under the specified temperature and then they were kept at this strain for 10 min. Subsequently, the force was removed from the samples suddenly and the remaining strain was measured as fixed strain, $\varepsilon_f$. After that for shape recovery measurement, the samples were heated up to 60 °C in 1 min and the final strain was recorded as recovery strain, $\varepsilon_r$. The aforementioned test was conducted for at least three specimens. The shape fixity ($R_f$) and the shape recovery ($R_r$) were calculated according to the following equations [13].

$$R_f = \frac{\varepsilon_f}{\varepsilon_m} \times 100\ \% \quad (1)$$

$$R_r = \frac{\varepsilon_m - \varepsilon_r}{\varepsilon_m} \times 100\ \% \quad (2)$$

Shape recovery temperature of the samples was measured by a thermal chamber equipped with a temperature controller, thermocouple and digital camera. The extended samples up to 200 % strain were placed in the designed chamber, then the temperature was increased up to 80 °C at a rate of 2°/min, and the images of deformed samples were captured individually at each temperature. The temperature at which the sample reaches to its ultimate shape was reported as shape recovery temperature.

## Results and discussion

### Characterization of synthesized PCL-diol and PUUs

PCL-diols with two different molecular weights (2000 and 4000 g/mol) were synthesized by stannous octoate catalyzed ring opening polymerization of ε-caprolactone in the presence of 1,4-butandiol as co-initiator. Experimental molecular weight of PCL-diols obtained from $^1$H NMR spectra shows a good agreement with calculated theoretical molecular weight, found from initial monomer concentration to initial co-initiator concentration ratios ($[CL]_0/[BD]_0$) (1983 vs. 2000).

PUUs were prepared by the aforementioned method. As shown in Table 1, six PUUs were synthesized with different HDI/PP/PCL-diol molar ratios (2/1/1, 3/2/1, and 5/4/1). In the resulting PUUs, PCL serves as the soft segment and the reaction product of HDI and PP forms the hard segment. The hard segment contents (HSC, expressed as percentage) of PUUs, calculated according to Eq. 3 [16], are presented in Table 1.

$$HSC = \frac{100 \times \left(n_{HDI} \times M_{HDI} + n_{pp} \times M_{PP}\right)}{n_{PCL} \times M_{PCL} + n_{HDI} \times M_{HDI} + n_{pp} \times M_{PP}}\ \%, \quad (3)$$

where $M_{PCL}$, $M_{HDI}$, $M_{PP}$ are the molecular weights and $n_{PCL}$, $n_{HDI}$, and $n_{PP}$ are the mole numbers of PCL, HDI, and PP, respectively.

### NMR analysis

$^1$H-NMR was used to characterize the chemical structure of PCL-diol and PUUs. As a representative for PCL-diols and PUUs, $^1$H NMR spectra of PCL-diol (Mn = 2000), PUU-4000-211 and detailed data on chemical shifts and associated protons in polymer chain, are presented in Fig. 1. For PCL-diol, resonances at 1.4 ($\delta_H^a$: –$CH_2$–$C\underline{H}_2$–$CH_2$–), 1.63–1.67 ($\delta_H^b$: –$C\underline{H}_2$–$CH_2$–O), 2.3–2.34 ($\delta_H^c$: $C\underline{H}_2COO$), and 4.046–4.09 ($\delta_H^e$: $C\underline{H}_2OCO$) are assigned to methylene protons in PCL repeating unit, respectively. The resonance at 3.65 ($\delta_H^d$: $C\underline{H}_2OH$) is related to protons in the terminal group of PCL-diol (Fig. 1a) [38]. These results are in agreement with proposed structure for PCL-diol. The molecular weight of PCL-diol was calculated from the ratio between –$C\underline{H}_2$–COO (4.046–4.09 ppm) and –$C\underline{H}_2$–OH

**Table 1** HSC, melting temperature, crystallization temperature, and degree of crystallinity of synthesized PUUs samples

| Sample | HSC (%) | $T_m$ (°C)[a] | $T_c$ (°C)[b] | $X_c$ (%)[c] | $X_c$ (%)[d] |
|---|---|---|---|---|---|
| PUU-2000-211 | 17.4 | 47.9 | −2.4 | 28.3 | 32.8 |
| PUU-2000-321 | 25.2 | 36.1 | −19.9 | 16.2 | 14.5 |
| PUU-2000-541 | 37.2 | 29.6 | −25.2 | 2.5 | 0.0 |
| PUU-4000-211 | 9.5 | 55.5 | 13.3 | 36.7 | 38.5 |
| PUU-4000-321 | 14.5 | 51.7 | 9.3 | 29.0 | 30.1 |
| PUU-4000-541 | 22.8 | 50.1 | 0.7 | 12.5 | 19.0 |

[a,c] Obtained from first heating run in DSC analysis

[b] Obtained from cooling run in DSC analysis

[d] Obtained from XRD patterns

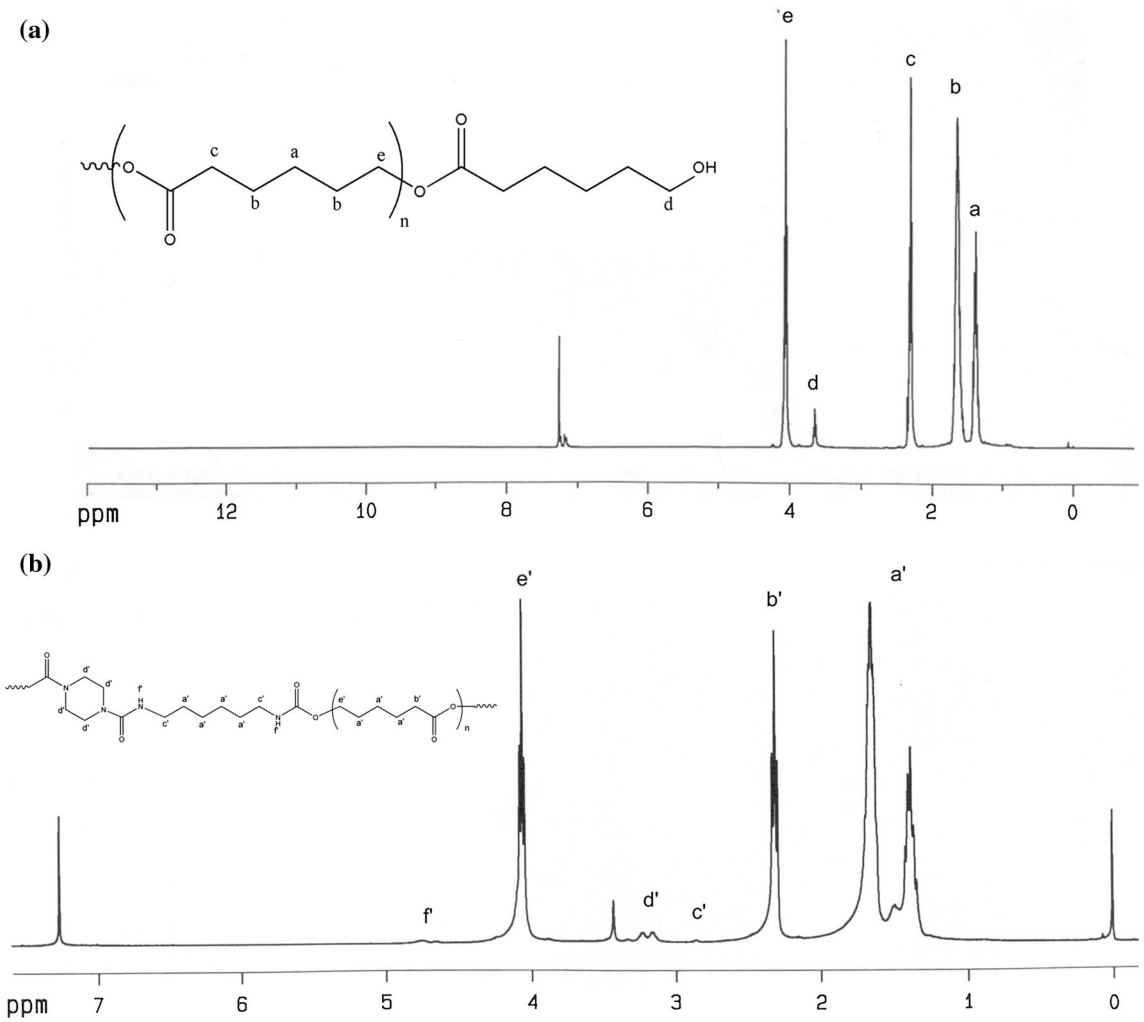


**Fig. 1** $^{1}$H NMR spectra of **a** PCL-2000 and **b** PUU-2000-211polymer

(3.65 ppm) resonances in $^{1}$H NMR spectra. The resulting molecular weights show good agreement with theoretical molecular weights (1983 vs. 2000 g/mol).

Moreover in $^{1}$H NMR spectra of PUU-2000-211, in addition to characteristic resonance of PCL, new characteristic resonances at 2.9 ppm ($\delta_H^{c'}$, $C\underline{H}_2NHCO$), 3.14–3.23 ppm ($\delta_H^{d'}$, protons in PP ring), and 4.75 ppm ($\delta_H^{f'}$, $N\underline{H}CO$) are observed which provide evidence for urethane and urea bond formation in polymer chain (Fig. 1b) [31, 35].

## FTIR analysis

FTIR spectroscopy was used to characterize the chemical structure of PUU samples. Figure 2 shows the ATR-FTIR spectra of PCL-2000 and PUU-2000 samples with various hard to soft segment ratios. The main characteristic absorption bonds observed in FTIR spectra are summarized in Table 2 [30, 35].

Comparing of PCL-diol and PUUs spectra showed that the characteristic bond at 3523 $cm^{-1}$ in PCL-diol (assigned to OH stretching vibration) is replaced by bond at 3353 in PUUs (assigned to NH stretching vibration). Also in the PUUs, two new bonds appear at 1620 (urea carbonyl stretching) and 1534 (amid II). These spectral changes provide conclusive evidence for polyurethane and urea bond formation in PUUs. Furthermore, the non-appearance of NCO absorption bond at around 2270 $cm^{-1}$ in FTIR spectra confirmed the absence of unreacted NCO groups and consequently confirmed the completion of the reaction.

As well as comparison of PUUs spectra showed no change in position of different bonds by changing HSC. However, variation of hard to soft segment ratio results in quantitative changes in some FTIR spectra bands. By increasing the hard to soft segment ratio, the intensity of the bonds at 1532 and 1620 $cm^{-1}$ increases, whereas the intensity of the band at 1189 $cm^{-1}$ decreases. These changes were attributed to increasing of urethane and urea

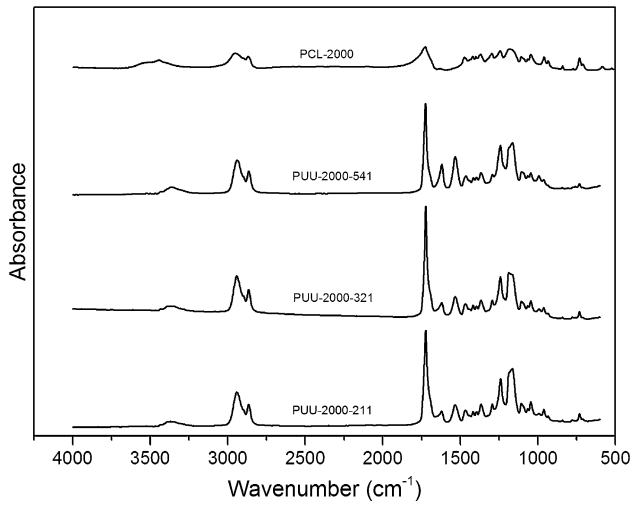


**Fig. 2** ATR-FTIR spectra of PCL-2000 and PUUs-2000 polymer

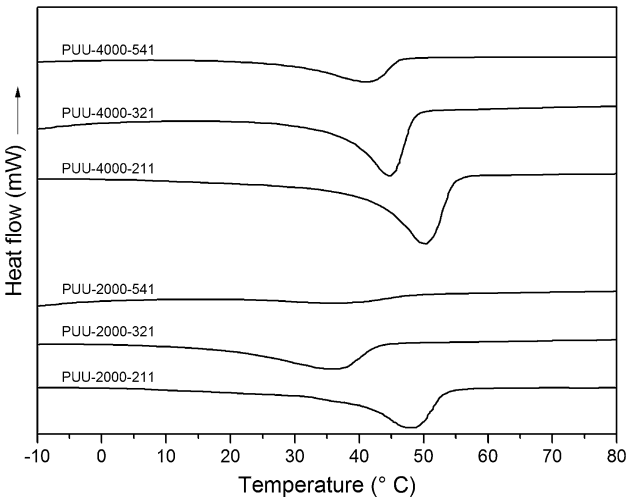


**Fig. 3** DSC thermograms of different PUU polymers

bond concentration with respect to ester group's concentration.

## Thermal properties

Thermal properties of PUUs were studied by DSC analysis. DSC thermograms of PUUs are shown in Fig. 3. All PUUs show a thermal transition which is related to melting temperature of PCL soft segment. Melting temperature ($T_m$) and degree of crystallinity ($X_c$) of PUUs are summarized in Table 1. As it can be seen in this table, $T_m$ and $X_c$ greatly depend both on PCL molecular weight and hard to soft segment ratio. Increasing of PCL molecular weight leads to higher $T_m$ and $X_c$. As well by increasing of HSC, $T_m$ and $X_c$ decrease, because hard segments have higher glass transition ($T_g$) value than crystallization temperature of PCL, so this difference can be attributed to the restriction of PCL crystallization by hard segments. Consequently, $T_m$ and $X_c$ of PUUs can be adjusted by controlling of PCL molecular weight and hard to soft segment ratio in appropriate range.

## Crystalline structure of synthesized PUUs

Figure 4 shows X-ray diffraction (XRD) patterns of the PUUs. In all PUUs except PUU-2000-541, the diffraction patterns are typical of semi-crystalline polymers. The main diffraction peaks located at $2\theta = 21.5°$, 22°, and 23.75° are related to the planes (110), (200), and (020) in the orthorhombic unit cell of PCL, respectively [15]. As a result, it can be concluded that the crystalline structure of PUUs originates from PCL soft segments. The degrees of crystallization of PUUs, obtained from XRD patterns, are presented in Table 1. In accordance to DSC results, it can be observed that the degree of crystallinity decreases with increasing of hard to soft segment ratio. This reduction can be attributed to hard segment restriction on PCL soft segment crystallization, mainly through strong hydrogen bonding interaction of soft and hard segment. However, diffraction pattern of PUU-2000-541, shows a broad amorphous halo near $2\theta = 20°$ which is typical of a non-crystalline state. In this sample HSC is high enough to restrict the soft PCL segment crystallization.

**Table 2** Main absorption bonds in ATR-FTIR spectra of PUUs [30, 35]

| Wave number ($cm^{-1}$) | Associated vibrations |
|---|---|
| 3200–3450 | Free and bonded N–H stretching vibration |
| 2800–3000 | $CH_2$ symmetric and anti-symmetric stretching vibration |
| 1600–1800 | C=O stretching vibration (amid I) |
| 1500–1590 | C–N stretching and N–H bending vibrations (amid II) |
| 1450–1490 | $CH_2$ scissoring, $CH_3$ deformation, and $CH_2$ bending |
| 1294 | C–N stretching with N–H bending vibrations of –R–NH–COO– (amid III) |
| 1239, 1168, and 1064 | Stretching vibrations of ester, –CO–O–C– group |
| 775 | Out-of plane bending of ester group |

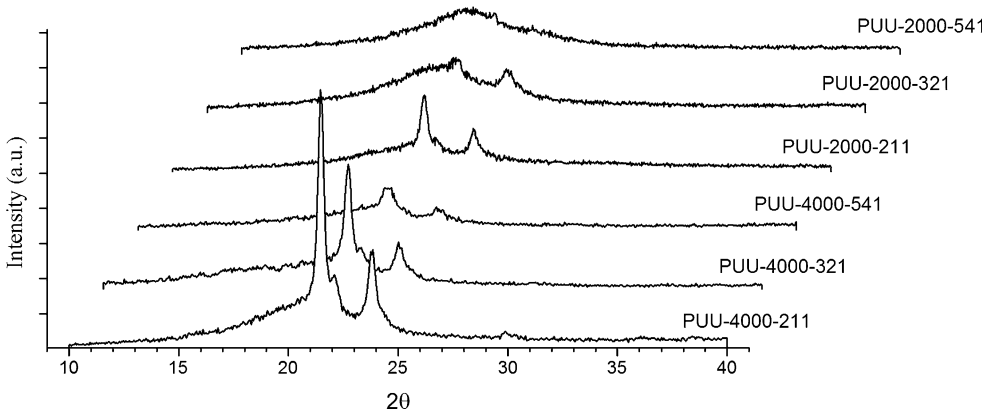


**Fig. 4** XRD patterns of different PUU polymers

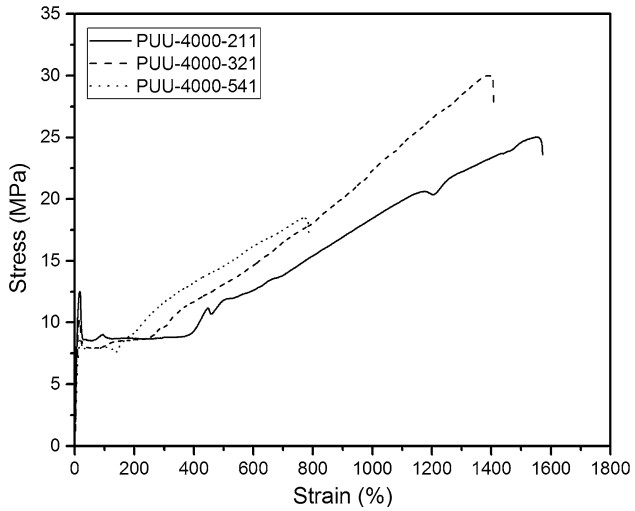


**Fig. 5** Stress-strain curves of different PUUs-4000 at room temperature

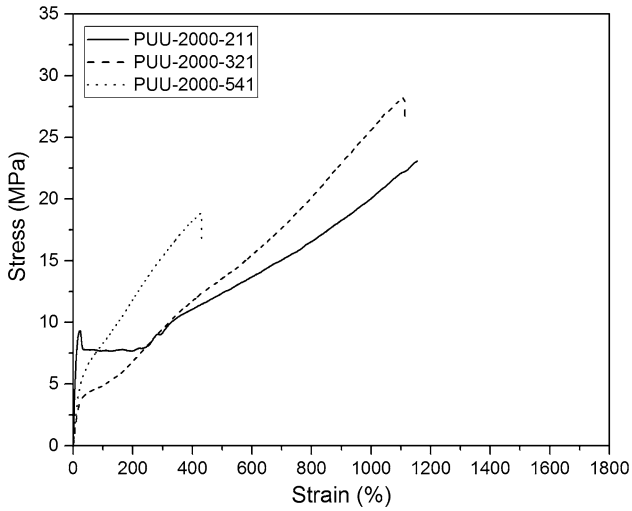


**Fig. 6** Stress-strain curves of different PUUs-2000 at room temperature

## Tensile properties

Tensile stress–strain curves of PUUs-2000 and PUUs-4000 samples at room temperature are compared in Figs. 5 and 6, respectively. Many factors influence the mechanical properties of PUUs. Soft segment molecular weight, degree of crystallinity, degree of phase separation, and HSC are the most important factors which must take into account in interpreting of tensile properties of PUUs [16, 17, 20, 32, 35]. PUUs-4000 and PUU-2000-211 show behavior typical for semi-crystalline polymers with non-homogeneous deformation characterized by necking and drawing, whereas PUU-2000-321 and PUU-2000-541 show behavior like highly cross-linked rubbers. The mechanical characteristics of PUUs are presented in Table 3. The yield strength for samples with homogenous deformation was defined as the stress in the intersection of the tangent at the origin with the tangent having the least slope. The results show that tensile modulus and yield strength of PUUs-4000 samples decrease with HSC increment. However in the case of PUUs-2000 samples, a noticeable reduction in tensile modulus and yield strength was observed in comparison of PUU-2000-321 and PUU-2000-541 with PUU-2000-211, but PUU-2000-541 shows higher tensile modulus and yield strength in respect to PUU-2000-321. As deduced from DSC and XRD examinations, the crystalline structure of PUUs originates from PCL soft segments. Moreover, it is realized that the PCL degree of crystallinity decreases with increasing of HSC. Consequently, by reduction of crystalline regions of the PCL soft segment which can serve as reinforcing agent, tensile modulus and yield strength reduce remarkably. However, it is ascertained that hard segments in PU and PUU act as physical cross-links and thus increase the Young modulus and tensile strength (filler effect) [18, 34, 35]. Thus in low crystalline PUU-2000-321 and PUU-2000-541, the effect of HSC dominates and tensile modulus and yield strength increase with HSC increment. In order to exclude HSC effect, tensile tests of PUUs are performed above the melting temperature of PCL soft segment (at 60 °C). The typical stress–strain curves are shown in Fig. 7. It can be observed

**Table 3** Mechanical properties of PUU samples, measured at room temperature

| Sample | Modulus (MPa) | Yield strength (MPa) | Elongation at break (%) | Onset of densification (%) |
|---|---|---|---|---|
| PUU-2000-211 | 61.0 ± 4 | 8.00 ± 1 | 1190 ± 17 | 240 ± 12 |
| PUU-2000-321 | 19.0 ± 0.5 | 4.00 ± 0.3 | 1124 ± 20 | 156 ± 3 |
| PUU-2000-541 | 22.7 ± 2 | 5.16 ± 0.4 | 455 ± 16 | 52 ± 3.6 |
| PUU-4000-211 | 109.0 ± 2 | 12.86 ± 1 | 1550 ± 30 | 389 ± 15 |
| PUU-4000-321 | 95.0 ± 1.5 | 10.46 ± 0.3 | 1444 ± 17 | 281 ± 23 |
| PUU-4000-541 | 84.0 ± 2 | 8.78 ± 0.35 | 770 ± 1.5 | 186 ± 41 |

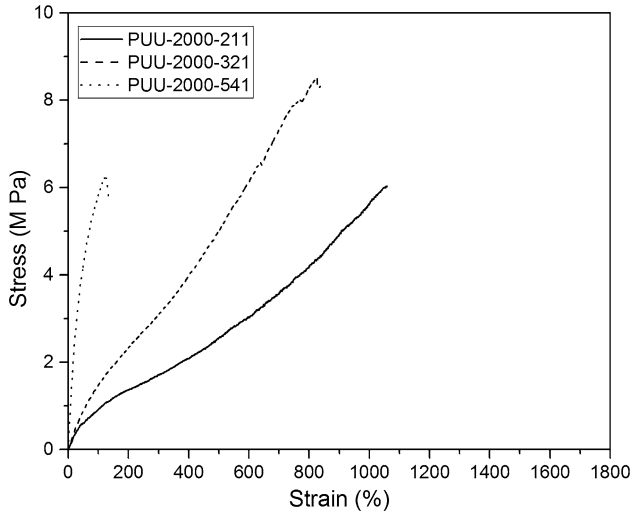


**Fig. 7** Stress–strain curves of different PUUs-2000 at 60 °C

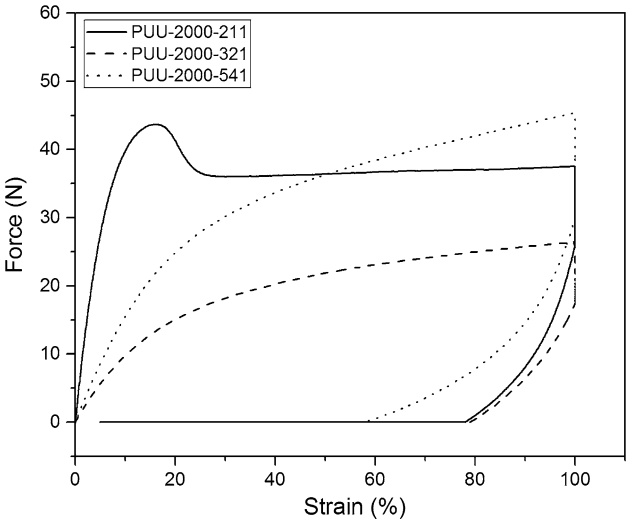


**Fig. 8** Force–strain curves of different PUUs-2000 obtained from shape memory process with initial deformation at room temperature

that tensile modulus and strength increase with increasing of HSC. Therefore, it can be concluded that, increasing of HSC has two opposite effects on mechanical properties. It may reduce mechanical properties by reduction of PCL soft segment crystallization, and on the other hand, it may improve mechanical properties through filler-like effect and probably higher molecular interaction with soft segments.

Elongation at break and strain at the onset of the densification zone are two other notable mechanical characteristics which differ greatly in PUUs. The results showed that the elongation at break and strain at the onset of densification zone decrease with HSC. It is known that increasing length of the network chains in single-phase polymer networks leads to increasing of the elongation at break [13]. Thus by assuming the segmented PUUs as a polymer network with hard segments as network points, this can be concluded that by increasing of soft segment content, the elongation at break increases.

## Shape memory properties of PUUs

Shape memory effect in PUUs arises from the ability of PCL soft segments to crystallize at room temperature. The hard segments composed of HDI and PP serve as physical cross-links which control the permanent shape of PUUs. Also phase separation due to thermodynamic incompatibility of soft and hard segments leads to the fact that each segment performs its distinct role in shape memory process. Shape memory properties including shape fixity and shape recovery were measured from two sets of thermo-mechanical cyclic tensile tests, mentioned above. Figures 8 and 9 show typical stress–strain curves in shape memory test for PUUs-2000, initially deformed at room temperature and 60 °C, respectively. The shape fixity and shape recovery of PUUs are compared in Table 4.

The results show that PUUs-4000 have approximately similar shape fixity around 80 % while they deformed at room temperature and over than 98 % as they deformed at 60 °C. However the shape fixity of PUUs-2000 shows dependency on HSC, particularly in PUU-2000-541 the shape fixity is reduced to 60 %. This trend which has also been shown by other researchers [27, 34], results from the PCL crystallization reduction with HSC increment. However the results reveal that the shape fixity of PUUs greatly depends on programming procedure in shape memory process. On the other hands, when the samples are

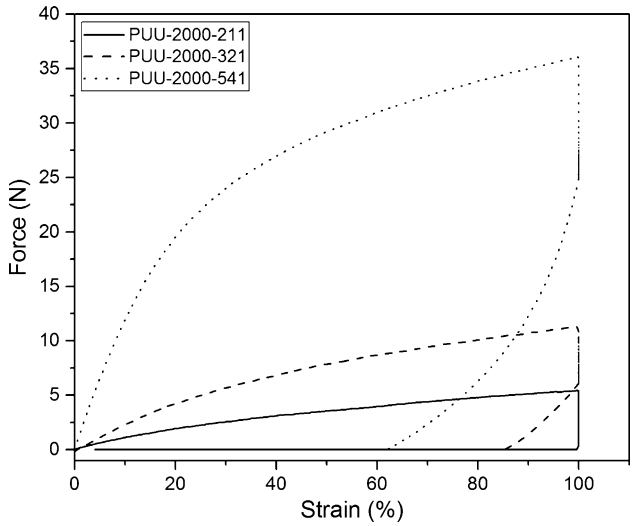


**Fig. 9** Force–strain curves of different PUUs-2000 obtained from shape memory process with initial deformation at 60 °C

deformed at room temperature, the shape fixity is lower than that they deformed at 60 °C. This difference in shape fixity may have two main explanations. First, while the samples deform at 60 °C which is over the melting temperature of PCL soft segments, the mobility of the chains increases and consequently the induced extension force reduces compared to the deformation at room temperature (for example 5.5 vs. 37.5 N for PUU-2000-211). As well as in the case of deformation at 60 °C, since PCL crystallization in PUUs is a time-dependent process, the chains have more mobility to relax extension force after fixing step. Thus the relaxation of retraction force induced by extension is high in samples which deformed at 60 °C compared to the samples deformed at room temperature, which eventually leads to better shape fixing. Secondly, crystalline morphology of PCL soft segments which formed during fixing step may be different in each programming procedure. In order to understand crystalline morphology changes of PCL soft segments, two sets of XRD tests were conducted on PUUs before deformation and after shape fixing step in both programming procedures. Figure 10 shows the typical shape fixing step in two aforementioned shape memorization processes. As discussed in XRD analysis, diffraction pattern of PUU-2000-541 shows no bonds associated to PCL crystals which indicate that the soft segment is completely amorphous. However, it can be seen that the diffraction peaks appear after shape fixing step. More interestingly the intensity of diffraction peaks is higher when the samples deformed at 60 °C. This observation reveals that more PCL crystals are formed during deformation at 60 °C which leads to higher shape fixity.

In addition as it can be seen, all of the PUUs, show shape recovery over 94 % in both programming procedures. Physically cross-linked network resulted from hard segments and their phase morphology determines the shape recovery of segmented PU and PUU. Ji et al. [17] showed that if phase morphology of hard segments in segmented PU changes from isolated to inter-connected state, a dramatic decrease in shape recovery occurs. They attributed this reduction to the unrecoverable plastic deformation built-up at hard segments in the extension. HSC in all of our synthesized PUUs is lower than 36 % which indicates probably the formation of isolated hard segment phase morphology. As a result, unrecoverable plastic deformation induced in hard segments is low enough in all of the PUUs to recover the majority of their original shapes (over 94 %). However, the results show that shape recovery reduces slightly with HSC which can be attributed to very small unrecoverable plastic deformation, developed at hard segments. In addition, samples deformed at 60 °C show lower shape recovery than samples deformed at room temperature. At 60 °C, the strength of hydrogen bonds between hard segments reduces, and so hard segments experience high deformation on extension which leads to lower shape recovery.

Shape recovery temperature in PUUs is related to melting temperature of PCL crystals. Thus as it can be seen in

**Table 4** Shape fixity, shape recovery, and shape recovery temperature of different PUU samples at various temperatures

| Sample | Room temperature | | 60 °C | | |
|---|---|---|---|---|---|
| | Shape fixity (%) | Shape recovery (%) | Shape fixity (%) | Shape recovery (%) | Recovery temperature (°C) |
| PUU-4000-211 | 84.6 ± 0.1 | 98.0 ± 0.1 | 99.3 ± 0.5 | 97.2 ± 0.3 | 65 |
| PUU-4000-321 | 83.5 ± 0.5 | 97.5 ± 0.2 | 99.0 ± 0.5 | 96.5 ± 0.2 | 60 |
| PUU-4000-541 | 80.5 ± 0.5 | 96.9 ± 0.3 | 98.5 ± 0.4 | 95.6 ± 0.2 | 56 |
| PUU-2000-211 | 78.0 ± 0.5 | 97.9 ± 0.1 | 98.3 ± 0.2 | 96.7 ± 0.1 | 49 |
| PUU-2000-321 | 76.7 ± 1 | 95.8 ± 0.2 | 84.0 ± 1 | 94.8 ± 0.3 | 46 |
| PUU-2000-541 | 57.8 ± 0.5 | 95.1 ± 0.1 | 60.0 ± 1 | 94.3 ± 0.2 | 40 |

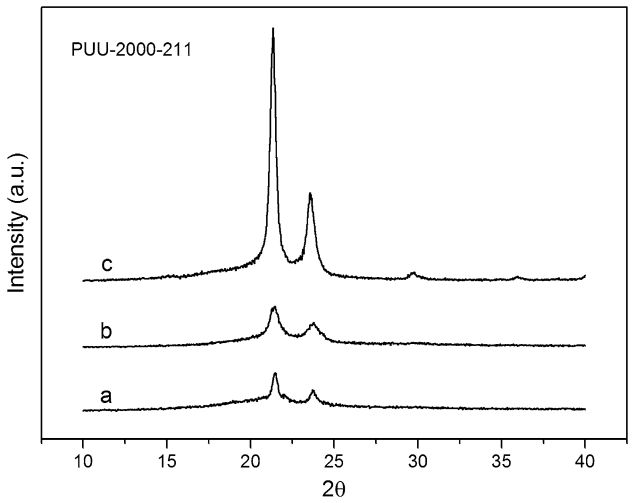


**Fig. 10** XRD pattern of PUU-2000-211; (*a*) before extension, (*b*) extended and fixed at room temperature, and (*c*) extended and fixed at 60 °C

Table 4, shape recovery temperature significantly depends on the PCL-diol molecular weight as well as HSC. By increasing of PCL-diol molecular weight, shape recovery temperature increases, which is probably due to the formation of more and perfect PCL crystal structure. However, by increasing of HSC which leads to lower degree of crystallinity, shape recovery temperature decreases.

## Conclusions

A series of biodegradable segmented PUU with significant shape memory properties were prepared using PCL soft segment and HDI-PP hard segment. HSC of samples was controlled by changing the molecular weight of PCL-diol as well as HDI/PP/PCL molar ratio. The results revealed that the crystalline structure of PUUs originate from PCL soft segment and shows a great dependency on HSC. Furthermore, it is concluded that the mechanical properties of PUUs depend on degree of crystallinity and HSC. Moreover, all PUUs independent from shape memory programming showed high shape recovery behavior. However, the samples which were deformed at 60 °C showed higher shape fixity than the samples were deformed at room temperature. The shape recovery temperature of PUUs can be controlled in the range of 40–65 °C by adjusting the PCL-diol molecular weight and the hard to soft segment ratio.

## References

1. Behl M, Lendlein A (2007) Shape-memory polymers. Mater Today 10:20–28
2. Behl M, Razzaq MY, Lendlein A (2010) Multifunctional shape-memory polymers. Adv Mater 22:3388–3410
3. Ratna D, Karger-Koscic J (2008) Recent advances in shape memory polymers and composites: a review. J Mater Sci 43:254–269. doi:10.1007/s10853-007-2176-7
4. Zhao Q, Behl M, Lendlein A (2013) Shape-memory polymers with multiple transitions: complex actively moving polymers. Soft Matter 9:1744–1755
5. Jiang H, Kelch S, Lendlein A (2006) Polymers move in response to light. Adv Mater 18:1471–1475
6. Lee HF, Yu HH (2011) Study of electroactive shape memory polyurethane–carbon nanotube hybrids. Soft Matter 7:3801–3807
7. Schmidt A (2006) Electromagnetic activation of shape memory polymer networks containing magnetic nanoparticles. Macromol Rapid Commun 27:1168–1172
8. Serrano MC, Ameer GA (2012) Recent insights into the biomedical applications of shape-memory polymers. Macromol Biosci 12:1156–1171
9. Lendlein A, Langer R (2002) Biodegradable, elastic shape-memory polymers for potential biomedical applications. Science 296:1673–1676
10. Lendlein A, Behl M, Hiebl B, Wischke C (2010) Shape-memory polymers as a technology platform for biomedical applications. Expert Rev Med Devices 7:357–379
11. Metcalfe A, Desfaits AC, Salazkin I, Yahia L, Sokolowski WM, Raymond J (2003) Cold hibernated elastic memory foams for endovascular interventions. Biomaterials 24:491–497
12. Small W, Wilson T, Benett W, Loge J, Maitland D (2005) Laser-activated shape memory polymer intravascular thrombectomy device. Opt Express 13:8205–8213
13. Petrovic ZS, Ferguson J (1991) Polyurethane elastomers. Prog Polym Sci 16:695–836
14. Kim BK, Lee SY (1996) Polyurethane having shape memory effects. Polymer 37:5781–5793
15. Kloss J, Munaro M, Souza GPD, Gulmint JV, Wang SH, Zawadzki S, Akcelrud L (2002) Poly(ester urethane)s with polycaprolactone soft segments: a morphological study. J Polym Sci, Part A 40:4117–4130
16. Ping P, Wang W, Chen X, Jing X (2005) Poly (ε-caprolactone) polyurethane and its shape-memory property. Biomacromolecules 6:587–592
17. Ji FL, Hu JL, Li TC, Wong YW (2007) Morphology and shape memory effect of segmented polyurethanes. Part I: with crystalline reversible phase. Polymer 48:5133–5145
18. Wang W, Ping P, Chen X, Jing X (2007) Biodegradable polyurethane based on random copolymer of L-lactide and ε-caprolactone and its shape-memory property. J Appl Polym 104:4182–4187
19. Krol P (2007) Synthesis methods, chemical structures and phase structures of linear polyurethanes. Properties and applications of linear polyurethanes in polyurethane elastomers, copolymers and ionomers. Prog Mater Sci 52:915–1015
20. He Y, Xie D, Zhang X (2014) The structure, microphase-separated morphology, and property of polyurethanes and polyureas. J Mater Sci 49:7339–7352. doi:10.1007/s10853-014-8458-y
21. Ping P, Wang W, Chen X, Jing X (2007) The Influence of hard-segments on two-phase structure and shape memory properties of PCL-based segmented polyurethanes. J Polym Sci, Part B 45:557–570
22. Korley LTJ, Pate BD, Thomas EL, Hammond PT (2006) Effect of the degree of soft and hard segment ordering on the morphology and mechanical behavior of semicrystalline segmented polyurethanes. Polymer 47:3073–3082
23. Gorna K, Polowinski S, Gogolewski S (2002) Synthesis and characterization of biodegradable poly (ε-caprolactone urethane)s. I. effect of the polyol molecular weight, catalyst, and

chain extender on the molecular and physical characteristics. J Polym Sci, Part A 40:156–170
24. Chen S, Hu J, Zhuo H, Chen S (2011) Effect of MDI–BDO hard segment on pyridine-containing shape memory polyurethanes. J Mater Sci 46:5294–5304. doi:10.1007/s10853-011-5469-9
25. Bogdanov B, Toncheva V, Schacht E, Finelli L, Sarti B, Scandola M (1999) Physical properties of poly(ester-urethanes) prepared from different molar mass polycaprolactone-diols. Polymer 40:3171–3182
26. Yang JH, Chun BC, Chung YC, Cho JH (2003) Comparison of thermal/mechanical properties and shape memory effect of polyurethane block-copolymers with planar or bent shape of hard segment. Polymer 44:3251–3258
27. Momtaz M, Razavi-Nouri M, Barikani M (2014) Effect of block ratio and strain amplitude on thermal, structural, and shape memory properties of segmented polycaprolactone-based polyurethanes. J Mater Sci 49:7575–7584. doi:10.1007/s10853-014-8466-y
28. Szycher M (1988) Biostability of polyurethane elastomers: a critical review. J Biomater Appl 3:297–402
29. Wang YL, Huang MN, Luo YF, Li YG (2010) In vitro degradation of poly (lactide-co-p-dioxanone)-based shape memory poly (urethane–urea). Polym Degrad Stab 95:549–556
30. Reddy TT, Kano A, Maruyama A, Takahara A (2010) Synthesis, characterization and drug release of biocompatible/biodegradable non-toxic poly(urethane urea)s based on poly(ε-caprolactone)s and lysine based diisocyanate. J Biomater Sci Polym Ed 21:1483–1502
31. Heijkantsa RGJC, Calcka RV, Tienenb TG, Groota JH, Bumab P, Penningsa AJ, Vethb RPH, Schouten AJ (2005) Uncatalyzed synthesis, thermal and mechanical properties of polyurethanes based on poly(ε-caprolactone) and 1,4-butane diisocyanate with uniform hard segment. Biomaterials 26:4219–4228
32. Hernandez LM, Sanchez FH, Ribelles JLG, Serra RS (2011) Segmented poly(urethane-urea) elastomers based on polycaprolactone: structure and properties. J Appl Polym Sci 119:2093–2104
33. Wang Y, Li Y, Luo Y, Huang M, Liang Z (2009) Synthesis and characterization of a novel biodegradable thermoplastic shape memory polymer. Mater Lett 63:347–349
34. Chun BC, Cho TK, Chung YC (2006) Enhanced mechanical and shape memory properties of polyurethane block copolymers chain-extended by ethylene diamine. Eur Polym J 42:3367–3373
35. Ruan C, Wang Y, Zhang M, Luo Y, Fu C, Huang M, Sun J, Hu C (2012) Design, synthesis and characterization of novel biodegradable shape memory polymers based on poly(D, L-lactic acid) diol, hexamethylene diisocyanate and piperazine. Polym Int 61:524–530
36. Ruan C, Hu N, Hu Y, Jiang L, Cai Q, Wang H, Pan H, Lu WW, Wang Y (2014) Piperazine-based polyurethane-ureas with controllable degradation as potential bone scaffolds. Polymer 55:1020–1027
37. Ruan C, Hu Y, Jiang L, Cai Q, Pan H, Wang H (2014) Tunable degradation of piperazine-based polyurethane ureas. J Appl Polym Sci 131:40527–40532
38. Storey RF, Sherman JW (2002) Kinetics and mechanism of the stannous octoate-catalyzed bulk polymerization of ε–caprolactone. Macromolecules 35:1504–1512
39. Crescenzi V, Manzini G, Calzolari G, Borr C (1972) Thermodynamics of fusion of poly-β-propiolactone and poly-ε-caprolactone. comparative analysis of the melting of aliphatic polylactone and polyester chains. Eur Polym J 8:449–463